Behavior of cell aggregates under force-controlled compression

Mathematics and Mechanics of Solids
Vol. , No. , 2013, pp.

Behaviour of cell aggregates under force-controlled compression.

C. Giverso[1] *, **L. Preziosi**[1]
[1] Department of Mathematics, Politecnico di Torino, Corso Duca degli Abruzzi 24, 10129 Torino, Italy

Abstract.

In this paper we study the mechanical behavior of multicellular aggregates under compressive loads and subsequent releases. Some analytical properties of the solution are discussed and numerical results are presented for a compressive test under constant force imposed on a cylindrical specimen. The case of a cycle of compressions at constant force and releases is also considered. We show that a steady state configuration able to bear the load is achieved. The analytical determination of the steady state value allows to obtain mechanical parameters of the cellular structure that are not estimable from creep tests at constant stress.

Key words: aggregate compression, living tissues mechanical behaviour, elasto-visco-plasticity, creep test

1. Introduction

The description of the mechanical response of soft biological tissues to external stimuli is a challenging task, both from the biological and the mathematical point of view. It has been experimentally observed that biological tissues show uncommon mechanical responses and thus they require mathematical tools different from the ones used for inert matter [6, 13]. Indeed, cellular aggregates are really complex materials, made of multiple subelements, characterized by a non-homogenous localization of mechanical properties inside them and a high hetereogeneity among them [21, 22]. The adhesion among cells is mediated by the expression and activation of cell adhesion molecules (CAMs), especially cadherins, which are the major CAMs responsible for cell-cell adhesion in vertebrate tissues. The up-regulation or down-regulation of such molecules is mediated by the activation of specific signalling pathways inside the cells. The action of such pathways may occur in response to biochemical stimuli, to genetic alteration or to external mechanical stimuli (mechanotransduction). The identification of pathways regulating cell behaviour is of fundamental importance in order to better understand the response of cells and cellular aggregates. However, due to the high complexity of living systems, their identification is not yet accomplished and thus the mechanical behavior of multicellular systems is still far from being understood.
Even without taking into account the high heterogeneities in cellular composition and the complex subcellular organization, instruments from "non-standard" mechanics are required while dealing with living systems. For instance, Ambrosi and Mollica [1, 2], applied the *theory for materials*

*Corresponding author. E-mail: chiara.giverso@polito.it

with evolving natural configurations, introduced in [16, 17, 18, 19], to successfully investigate cell aggregate growth and remodelling (see [4] for a review).

Referring to the available literature, multicellular aggregates have been studied both from the experimental [7, 8, 9, 12, 23] and the mathematical [1, 2, 3, 13, 14] point of view. In particular, in [7, 8, 9] a fixed compressive deformation is applied to a cell aggregate and the stress exerted by the living material on the upper plate is recorded, whereas in [12] a dense cell suspension is subjected to shear. In [3, 13, 14] the authors proposed a model able to explain the phenomena observed during these compression experiments, using the concept that the natural configuration evolves, due to the rearrangement of adhesion bonds among cells, when the stress inside the aggregate becomes too high. In fact, this reorganization generates a plastic deformation. In [10] the viscous contribution of the liquid, filling void spaces among cells, was introduced in order to fit the stress-free evolutions of spheroids, observed in [7, 8, 9]. Indeed, when the imposed deformation is removed, these biological tests show that the shape recovery of aggregates is not instantaneous, as predicted in the models used in [1, 2, 3, 13, 14]. The model proposed in [10] is, instead, able to predict the stress-release dynamics along with pressure controlled experiments (e.g. creep test), that can not be fully explained with the models in [3, 13]. However, only the case in which the applied stress is maintained constant is presented in [10].

In order to compare the mathematical model with experiments that can be easily performed on aggregates, it is easier to apply a constant force rather than a constant stress. Indeed the applied force can be easily controlled in biological experiments. Moreover, as the aggregate is compressed, the transverse section of the sample increases and thus the constant force is distributed over a bigger area and the stress is no longer constant. In this work, we show that this leads to the achievement of a steady state configuration able to bear the load, differently from what shown in [10], in which the assumption of constant stress leads to the total disruption of the aggregate when the external stress is above the threshold that induces the internal reorganization of the aggregate structure. The analytical determination of the steady state value allows to determine mechanical parameters of the cellular structure that are not estimable from creep tests at constant stress.

Thus the aim of this work is to study the capability of aggregates to reorganize in order to bear an external load. In Section 2 we present the equations (adapted from [10]) that describe the deformation and reorganization of a cylindrical sample of a soft biological material under a homogeneous compressive force directed along the z-axis, $F_{appl}(t)$. Some properties of the solution are proved and numerical results are presented in Section 3 both for a single compression test and for a cycle of compressive constant forces and subsequent releases, making a comparison with the results obtained in [10] for a creep test under constant stress.

2. Model formulation

A biphasic mixture consisting of a solid and a fluid phase is perhaps the most essential model of multicellular aggregates [1, 2, 5, 11, 15]. Cells and the network of fibers form the solid elastic skeleton of the mixture, whereas the fluid phase stands for the interstitial fluid, that completely saturates the pores of the solid and may move throughout it.

Therefore, the multicellular aggregate is treated as a saturated porous medium, in which cells are characterized by the volume fraction ϕ_c and the liquid is described by the liquid volume fraction $\phi_\ell = 1 - \phi_c$.
The mathematical model describing the response of a soft biological specimen, treated as a porous medium, to a uniaxial compression test is described in [10], using the theory for materials with evolving natural configurations [16, 17, 18, 19].
According to that theory, we identify with $\mathbf{F}_n$ the deformation without cell reorganization (describing how the body is deforming locally while going from the natural configuration $\mathscr{B}_n$ to the actual configuration $\mathscr{B}_t$) whereas with $\mathbf{F}_p$ we refer to the anelastic component due to the internal re-organization of cells (evolution from the initial configuration $\mathscr{B}_0$ to $\mathscr{B}_n$). The multiplicative decomposition

$$\mathbf{F} = \mathbf{F}_n \mathbf{F}_p \,, \tag{2.1}$$

holds.
Under the hypothesis of a homogeneous uniaxial compression, satisfying

$$x = \frac{X}{\sqrt{\varphi(t)}},\; y = \frac{Y}{\sqrt{\varphi(t)}},\; z = \varphi(t) Z \,,$$

the deformation gradient from the initial to the final configuration is given by

$$\mathbf{F} = \text{diag}\left\{ \frac{1}{\sqrt{\psi(t)}}, \frac{1}{\sqrt{\psi(t)}}, \psi(t) \right\} , \tag{2.2}$$

where ψ is the stretch along the direction of compression (sometimes called deformation in the following for sake of simplicity).
The deformation gradient associated to the internal reorganization can be represented by

$$\mathbf{F}_p = \text{diag}\left\{ \frac{1}{\sqrt{\Psi_p(t)}}, \frac{1}{\sqrt{\Psi_p(t)}}, \Psi_p(t) \right\} , \tag{2.3}$$

where $\Psi_p(t)$ is a measure of how much the aggregate has reorganized and the natural configuration has evolved. We observe that for $\Psi_p(t) = 1$ we have no contribution due to rearrangement of bonds inside the body.
We assume that the cellular component obeys a neo-Hookean law, with coefficient of the isotropic term $-\Sigma_c(\phi_c)$ and shear modulus μ, and that the viscous liquid, characterized by kinematic viscosity ν, moves with the same velocity of the solid. Thus the constitutive part of the Cauchy stress tensor of the cellular constituent, $\mathbf{T}_c$, and of the liquid, $\mathbf{T}_\ell$, is given by

$$\mathbf{T}_c = -\Sigma_c(\phi_c)\mathbf{I} + \mu \mathbf{B}_n \,, \tag{2.4}$$

$$\mathbf{T}_\ell = 2\nu \mathbf{D} \,, \tag{2.5}$$

being $\mathbf{B}_n = \mathbf{F}_n\mathbf{F}_n^T$ and $\mathbf{D} = \dfrac{1}{2}(\mathbf{L} + \mathbf{L}^T)$ the symmetric part of the velocity gradient, $\mathbf{L} = \dot{\mathbf{F}}\mathbf{F}^{-1}$. The total stress exerted by the specimen, $\mathbf{T}_m$, neglecting inertial terms, is

$$\mathbf{T}_m = -p\mathbf{I} + \phi_c\mathbf{T}_c + \phi_\ell\mathbf{T}_\ell = -\left(p + \phi_c\Sigma_c(\phi_c)\right)\mathbf{I} + \mu\phi_c\mathbf{B}_n + 2(1-\phi_c)\nu\mathbf{D}\,. \tag{2.6}$$

For what concerns the description of plastic contribution, we refer to [13], where the rearrangement of cells during the deformation of a multicellular spheroids is related to the existence of a yield condition in the macroscopic constitutive equation of the stress tensor. Thus, the plastic evolution is described by the following equation [10, 13], linking the velocity gradient associated with the internal reorganization, $\mathbf{L}_p = \dot{\mathbf{F}}_p\mathbf{F}_p^{-1}$, to the deviatoric part of the Cauchy stress tensor of the cellular constituent, $\mathbf{T'}_c = \mathbf{T}_c - \frac{1}{3}\mathrm{tr}(\mathbf{T}_c)\mathbf{I}$,

$$\mathbf{L}_p = \mathbf{D}_p = \frac{\phi_c}{2\eta(\phi_c)}\left[1 - \frac{\tau(\phi_c)}{f(\phi_c\mathbf{T'}_c)}\right]_+ sym\left(\mathbf{F}_n^T\mathbf{T'}_c\mathbf{F}_n^{-T}\right)\,. \tag{2.7}$$

In (2.7) it is postulated the existence of a maximum stress, $\tau(\phi_c)$, that can be sustained by the cell aggregate before reorganizing. Indeed, if a proper measure of the stress, $f(\phi_c\mathbf{T'}_c)$ is below the stress $\tau(\phi_c)$ no remodelling occurs inside the aggregate and thus the body deforms elastically, whereas if this threshold is overcome, the cellular body undergoes an internal reorganization which can be modelled at a macroscopic level as a visco-plastic deformation. Considering that in the uniaxial compression test, the total force is applied in the z-direction, the following balance holds

$$\mathbf{T}_m = \mathrm{diag}\left\{0, 0, -P_{appl}(t)\right\}\,. \tag{2.8}$$

In a creep test at constant force, $P_{appl}(t) = F_{appl}(t)/S_{appl}(t) > 0$ is known in the compressive phase and it vanishes in the stress release phase.
Being $\mathbf{B}_n = \mathrm{diag}\left\{\dfrac{\Psi_p(t)}{\psi(t)}, \dfrac{\Psi_p(t)}{\psi(t)}, \dfrac{\psi^2(t)}{\Psi_p^2(t)}\right\}$ and $\mathbf{D} = \mathrm{diag}\left\{-\dfrac{1}{2}, -\dfrac{1}{2}, 1\right\}\dfrac{\dot{\psi}(t)}{\psi(t)}$, from (2.6) and (2.8) we obtain the following equation representing the evolution of the stretch of the aggregate

$$\frac{\dot{\psi}}{\psi} \;=\; -\frac{P_{appl}}{3\nu(1-\phi_c)} + \frac{\mu\phi_c}{3\nu(1-\phi_c)}\frac{\Psi_p^3 - \psi^3}{\psi\Psi_p^2}\,, \tag{2.9}$$

where we omit the dependence from t for sake of simplicity. Equation (2.9) can still be used to model the stress-free evolution of the system, imposing $P_{appl} = 0$.
Equation (2.9) needs to be joined with equation (2.7), taking into account that

$$\mathbf{T'}_c = \mu\,\mathrm{diag}\left\{-\frac{1}{3}, -\frac{1}{3}, \frac{2}{3}\right\}\frac{\psi^3 - \Psi_p^3}{\Psi_p^2\psi}\,. \tag{2.10}$$

and

$$\mathbf{L}_p = \mathrm{diag}\left\{-\frac{1}{2}, -\frac{1}{2}, 1\right\}\frac{\dot{\Psi}_p}{\Psi_p}\,. \tag{2.11}$$

and postulating an equation for $f(\phi_c \mathbf{T}'_c)$.
Here we consider that the frame invariant measure of the stress is the maximum shear stress magnitude, given by half of the difference between the maximum and the minimum stress in the principal directions (Tresca's criterion)

$$f(\phi_c \mathbf{T}'_c) = \frac{\mu\phi_c}{2} \frac{|\Psi_p^3 - \psi^3|}{\psi\Psi_p^2} \,, \tag{2.12}$$

. Under the assumptions stated above, the evolution of the internal reorganization is given by

$$\frac{\dot{\Psi}_p}{\Psi_p} = -\frac{1}{3\lambda}\left[1 - \frac{2\tau}{\mu\phi_c}\frac{\psi\Psi_p^2}{|\Psi_p^3 - \psi^3|}\right]_+ \frac{\Psi_p^3 - \psi^3}{\psi\Psi_p^2} \,. \tag{2.13}$$

where $\lambda = \dfrac{\eta(\phi_c)}{\mu\phi_c}$ is the *cell-reorganization time* (or plastic rearrangement time) and $\tau = \tau(\phi_c)$.
Thus the following system holds for a uniaxial compression test, with given applied stress P_{appl}

$$\dot{\psi} = -\frac{P_{appl}}{3\nu(1-\phi_c)}\psi + \frac{\mu\phi_c}{3\nu(1-\phi_c)}\frac{\Psi_p^3 - \psi^3}{\Psi_p^2} \,, \tag{2.14}$$

$$\dot{\Psi}_p = -\frac{1}{3\lambda}\left[\frac{\Psi_p^3 - \psi^3}{\psi\Psi_p^2} - \frac{2\tau}{\mu\phi_c}\right]_+ \mathrm{sgn}\,(\Psi_p - \psi)\Psi_p \,. \tag{2.15}$$

In particular, in [10], this model is applied to the description of cycles of compression and releases under constant deformation and constant stress.
In this paper we start from the observation that the control in the compression experiment is usually on the applied force that is related to the applied stress through $P_{appl}(t) = F_{appl}(t)/S_{appl}(t)$, where $S_{appl}(t)$ is the surface on which the load is applied that increases in time as the specimen is compressed. In order to define the external applied stress we need to do some hypothesis on the geometry of the biological sample. In this case we assume a cylindrical sample of soft biological material, thus, due to the definition of $\mathbf{F}$, we have

$$P_{appl}(t) = \frac{F_{appl}(t)\psi(t)}{\pi R_0^2} \,,$$

where R_0 is the initial radius of the sample.

In the following we state two propositions that are useful to analytically study the behaviour of the solution of the system (2.14)-(2.15). The first proposition allows to eliminate the $\mathrm{sgn}(\cdot)$ in (2.15).

Proposition 1. *When the aggregate is compressed with any sequence of compressive loads,* $F_{appl}(t) > 0$, *for* $t \in [t_{2i}, t_{2i+1}]$ *followed by stress release for* $t \in [t_{2i+1}, t_{2(i+1)}]$, *with* $i = 0, ..., n$, *if* $\Psi_p(0) \geq \psi(0)$, *then* $\Psi_p(t) \geq \psi(t), \forall t > 0$.

The proof follows the same steps used in [10] (Proposition 1), observing that $P_{appl}(t) = F_{appl}(t)/S_{appl}(t) > 0$, as compressive forces are positive.
Using Proposition 1, scaling times with 3λ and introducing the dimensionless quantities

$$\tilde{\tau} = \frac{2\tau}{\mu\phi_c}\,, \qquad \tilde{\mu} = \frac{\mu\lambda\phi_c}{\nu(1-\phi_c)}\,, \qquad \tilde{F}(t) = \frac{F_{appl}(t)}{\pi R_0^2 \mu\phi_c}\,,$$

the system (2.14)-(2.15) can be written in dimensionless form as

$$\begin{cases} \dot{\psi} = \tilde{\mu}[h(\Psi_p,\psi) - \tilde{F}(t)]\psi^2\,, \\ \\ \dot{\Psi}_p = -[g(\Psi_p,\psi) - \tilde{\tau}]_+\Psi_p\,, \end{cases} \tag{2.16}$$

where

$$h(\Psi_p,\psi) := \frac{\Psi_p^3 - \psi^3}{\Psi_p^2\psi^2}\,, \qquad g(\Psi_p,\psi) := \frac{\Psi_p^3 - \psi^3}{\Psi_p^2\psi} = h(\Psi_p,\psi)\psi\,. \tag{2.17}$$

It can be readily noticed that, for $(\psi,\ \Psi_p) \in [0,1]\times[0,1]$, both g and h are decreasing functions of ψ for fixed Ψ_p and increasing functions of Ψ_p for fixed ψ.
In order to examine the existence of stationary configurations, it will also be useful to define by $\psi_y(\Psi_{p,0})$ the unique value that inverts $g = \tilde{\tau}$ with respect to ψ for fixed $\Psi_p = \Psi_{p,0}$, i.e., such that

$$g(\Psi_{p,0},\psi_y(\Psi_{p,0})) = \frac{\Psi_{p,0}^3 - \psi_y^3(\Psi_{p,0})}{\Psi_{p,0}^2\psi_y(\Psi_{p,0})} = \tilde{\tau}\,, \tag{2.18}$$

so that the r.h.s. of the second equation in (2.16) vanishes. Similarly, we define $\psi_c(\Psi_{p,0})$ as the unique value that inverts $h = \tilde{F}_M = \max_t\{\tilde{F}(t)\}$ with respect to ψ for fixed $\Psi_p = \Psi_{p,0}$, i.e., such that

$$h(\Psi_{p,0},\psi_c(\Psi_{p,0})) = \frac{\Psi_{p,0}^3 - \psi_c^3(\Psi_{p,0})}{\Psi_{p,0}^2\psi_c^2(\Psi_{p,0})} = \tilde{F}_M\,, \tag{2.19}$$

so that the r.h.s. of the first equation in (2.16) vanishes.

The proposition proved in the following will be useful to define the yield condition in the case of experiments under imposed bounded force and the long time behaviour of the solution.

Proposition 2. *For any given* $\Psi_{p,0}$

$$\psi_y(\Psi_{p,0}) \le \psi_c(\Psi_{p,0}) \qquad \Longleftrightarrow \qquad \tilde{F}_M \le \frac{\tilde{\tau}}{\psi_y(\Psi_{p,0})}\,. \tag{2.20}$$

If $\tilde{F}_M > \dfrac{\tilde{\tau}}{\psi_y(1)}$ *the unique solution of the system*

$$\begin{cases} g(\Psi_p,\psi) = \tilde{\tau}\,, \\ h(\Psi_p,\psi) = \tilde{F}_M\,, \end{cases} \tag{2.21}$$

in $(0,1]^2$ *is* $\psi = \tilde{\tau}/\tilde{F}_M$ *and* Ψ_p *such that*

$$h\left(\Psi_p, \frac{\tilde{\tau}}{\tilde{F}_M}\right) = \tilde{F}_M\,. \tag{2.22}$$

Proof. Since h is a decreasing function of φ, if $\varphi_y(\Psi_{p,0}) \leq \varphi_c(\Psi_{p,0})$,

$$\tilde{F}_M = h(\Psi_{p,0}, \varphi_c(\Psi_{p,0})) \leq h(\Psi_{p,0}, \varphi_y(\Psi_{p,0})) = \frac{g(\Psi_{p,0}, \varphi_y(\Psi_{p,0}))}{\varphi_y(\Psi_{p,0})} = \frac{\tilde{\tau}}{\varphi_y(\Psi_{p,0})}\,.$$

Viceversa, if $\tilde{F}_M \leq \dfrac{\tilde{\tau}}{\varphi_y(\Psi_{p,0})}$, we have

$$h(\Psi_{p,0}, \varphi_y(\Psi_{p,0})) = \frac{g(\Psi_{p,0}, \varphi_y(\Psi_{p,0}))}{\varphi_y(\Psi_{p,0})} = \frac{\tilde{\tau}}{\varphi_y(\Psi_{p,0})} \geq \tilde{F}_M = h(\Psi_{p,0}, \varphi_c(\Psi_{p,0}))$$

and because of the fact that h is a decreasing function of φ, we can conclude that $\varphi_y(\Psi_{p,0}) \leq \varphi_c(\Psi_{p,0})$. On the other hand, for small ψ and Ψ_p it is possible to prove that the curve $h(\Psi_p, \psi) = \tilde{F}_M$ behaves like

$$\psi = \Psi_p - \frac{\tilde{F}_M}{3}\Psi_p^2\,,$$

while $g(\Psi_p, \psi) = \tilde{\tau}$ behaves like

$$\psi = \alpha\Psi_p\,, \quad \text{with} \quad \alpha < 1\,, \quad \text{solution of} \quad \alpha^3 + \tilde{\tau}\alpha - 1 = 0\,.$$

This means that in the square $(0,1]^2$ of the plane (Ψ_p, ψ), for small Ψ_p, the implicit curve $g(\Psi_p, \psi) = \tilde{\tau}$ always starts below $h(\Psi_p, \psi) = \tilde{F}_M$ and ends (at $\Psi_p = 1$) below or above according to the criterium (2.20) (see Fig. 1). Hence, if $\tilde{F}_M > \dfrac{\tilde{\tau}}{\psi_y(1)}$ there is at least a solution of (2.21). Uniqueness can be readily realized by observing that $g = h\psi$ and thus, substituting in the equations (2.16) the value $\psi = \tilde{\tau}/\tilde{F}_M$, Ψ_p is given by the solution of

$$h\left(\Psi_p, \frac{\tilde{\tau}}{\tilde{F}_M}\right) = \tilde{F}_M\,,$$

which is unique due to the monotonicity of h. □

3. Results and Discussion

In this section some analytical properties of the solution of the system (2.14)-(2.15) are stated and proved, along with simple simulations that clarify the behaviour of the aggregate subjected to an external load.

Numerical results are shown in the case of a single compression under constant force and in the case of a cycle of compression under constant force and subsequent release. However, we remark that the model presented can be used also to simulate also mechanical tests with applied force varying in time.

Therefore, analytical results are generalized to the case of a bounded force depending on time,

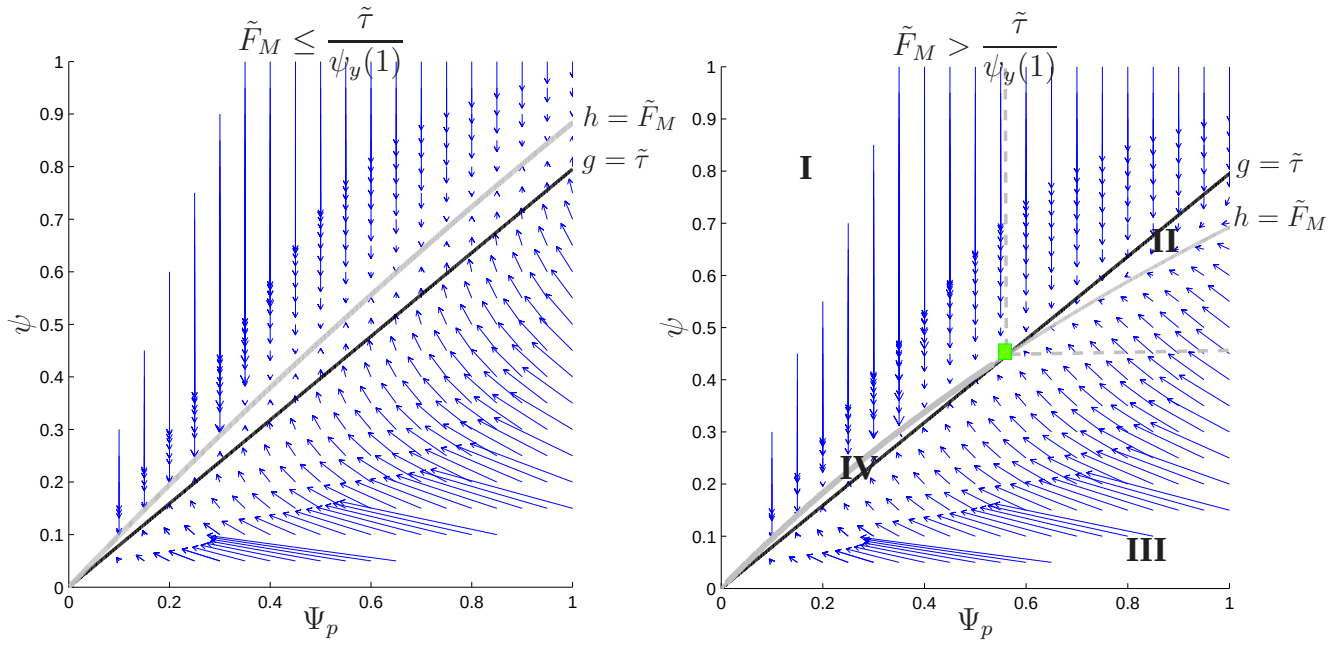

Figure 1: Vector field (arrows) corresponding to (2.16), if $\tilde{F}_M \leq \tilde{\tau}/\psi_y(1)$ (on the left) and $\tilde{F}_M > \tilde{\tau}/\psi_y(1)$. The black curve corresponds to $g(\Psi_p, \psi) = \tilde{\tau}$, i.e., $\psi_y(\Psi_p)$ whereas the grey curve to $h(\Psi_p, \psi) = \tilde{F}_M$, i.e., $\psi_c(\Psi_p)$. If $F_{appl}(t) \leq \tilde{F}_M \leq \tilde{\tau}/\psi_y(1)$, the trajectories will tend toward the grey curve. On the other hand, if $\tilde{F}_M > \tilde{\tau}/\psi_y(1)$, trajectories starting from $\psi = \Psi_p = 1$ will tend to the the intersection of the two curves (square mark), which represents the solution of the system (2.16). The gray curve delimiting region IV is thicker because is composed of non-isolated stationary points.

where possible.

Fig. 2 shows the results for a cyilindrical specimen of living material subjected to a single compression at constant force (solid curve) and constant stress (dashed curve), able to trigger the internal reorganization. In the case of a constant force, the axial deformation progressively increases, as the aggregate reorganize. A stable deformed configuration able to bear the external load is achieved even when internal reorganization occurs (see solid curve in Fig. 2).

Conversely, when the aggregate is deformed with a constant stress able to trigger the internal reorganization, the aggregate's remodelling continues until the multicellular body is totally squeezed between the upper and the lower plate (see dashed curve in Fig. 2). Indeed, if the applied stress applied to the specimen is initially above the yield condition and it is maintained constant in time, then the frame invariant measure of the stress in (2.3) is always above the threshold that induces internal reorganization. Thus remodelling continues until all bonds among cells are broken and the aggregate is totally disrupted. On the other hand if the applied initial force is able to induce the internal reorganization, as the aggregate reorganizes and deforms, the applied stress is no longer constant (due to the increasing transverse section) and a stationary deformation is reached.

The value of the stationary stretch is discussed in Corollary 6.

The following proposition focuses on the cases in which remodelling does not occurs. We observe that initially in the experiments $\psi(0) = \Psi_p(0) = 1$, because simulations starts with an

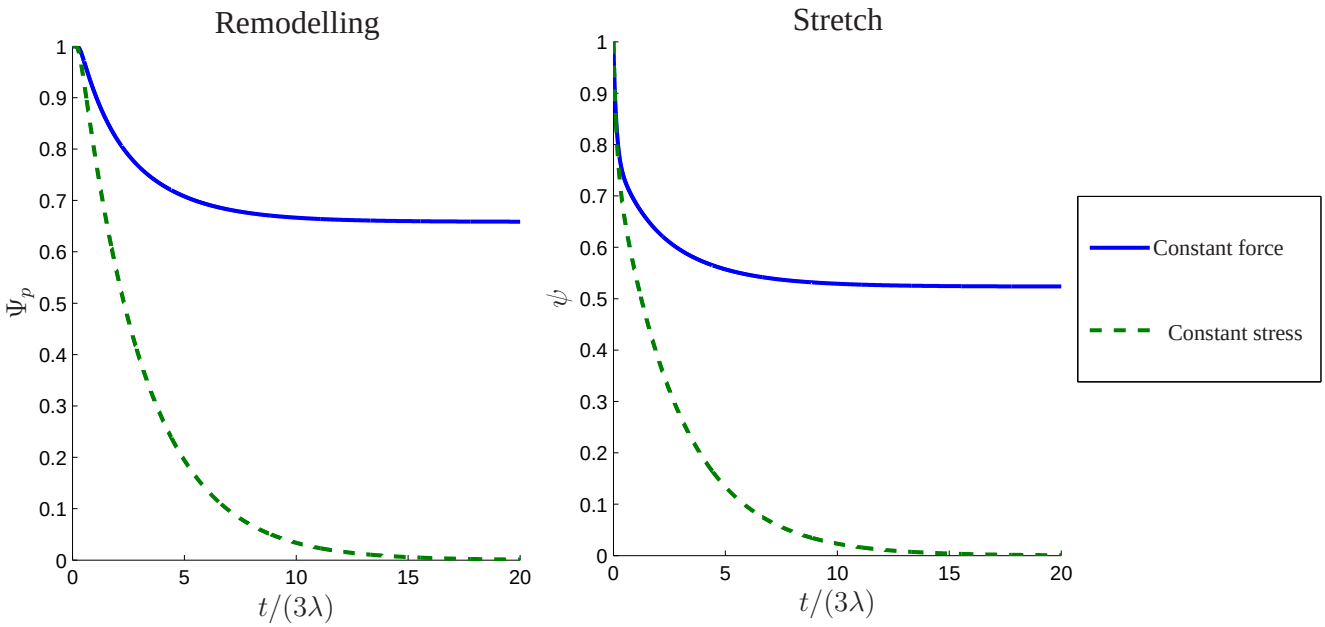

Figure 2: Compressions of a cylindrical sample, when a constant external force $\tilde{F}_M$ (solid curve) and when a constant stress (dashed curve) are applied: reorganization (on the left) and stretch (on the right). The simulations are performed setting the same initial stress on the cylindrical specimen of initial radius $R = 1mm$ ($\tilde{F}(t=0) = -1.1937$ and $\tilde{P}(t=0) = \dfrac{P_{appl}}{\pi\mu\phi_c} = -1.1937$), whereas $\tilde{\tau} = 0.625$ and $\tilde{\mu} = 1.6$.

undeformed aggregates, in which no remodelling has occurred. However, we generalize the statement to any $\Psi_p(0) = \Psi_{p,0} \geq \psi_0$, because the result will be useful for the discussion after Corollary 4.

Proposition 3. *If $\psi(0) = \psi_0 > \psi_c(\Psi_{p,0})$ and $\Psi_p(0) = \Psi_{p,0} \geq \psi_0$, applying a constant force $\tilde{F}(t) = \tilde{F}_M \leq \tilde{\tau}/\psi_y(\Psi_{p,0})$, $\forall t \geq 0$, then $\Psi_p(t) = \Psi_{p,0}$, $\forall t$ and the solution of Eq. (2.14), is such that $\psi(t) \geq \psi_c(\Psi_{p,0}) \geq \psi_y(\Psi_{p,0})$.*

Proof. First of all, being $\tilde{F}_M \leq \tilde{\tau}/\psi_y(\Psi_{p,0})$, from (2.20), we have $\psi_0 > \psi_c(\Psi_{p,0}) \geq \psi_y(\Psi_{p,0})$. Thus the following relations hold

$$h(\Psi_{p,0}, \psi_0) - \tilde{F}(0) < h(\Psi_{p,0}, \psi_c(\Psi_{p,0})) - \tilde{F}_M = 0\,,$$

$$\text{and } \; g(\Psi_{p,0}, \psi_0) - \tilde{\tau} < g(\Psi_{p,0}, \psi_y(\Psi_{p,0})) - \tilde{\tau} = 0\,,$$

because both g and h are decreasing functions of ψ for fixed Ψ_p. Then $\dot{\Psi}_p(0) = 0$, while ψ initially decreases. Actually $\Psi_p(t) = \Psi_{p,0}$ until ψ eventually reaches $\psi_y(\Psi_{p,0})$. If this value is overcome, then the material yields and Ψ_p can only decrease (see region II in Fig. 1, right panel).
However, we will now prove that $\psi(t)$ does not decrease below $\psi_c(\Psi_{p,0}) > \psi_y(\Psi_{p,0})$, so the material never yields and $\Psi_p(t) = \Psi_{p,0}$, $\forall t$.
To demonstrate that $\psi(t) \geq \psi_c(\Psi_{p,0})\,, \forall t > 0$, we define $w = \psi - \psi_c(\Psi_{p,0})$ and recalling that

$\psi_0 > \psi_c(\Psi_{p,0})$, so that $w_-(0) = 0$, we have

$$0 \geq -\frac{w_-^2(\tilde{t})}{2} = \int_0^{\tilde{t}} \dot{w} w_- dt = \int_0^{\tilde{t}} \tilde{\mu} \left[h(\Psi_{p,0}, \psi) - h(\Psi_{p,0}, \psi_c(\Psi_{p,0})) \right] \psi^2 w_- dt \,.$$

Then the r.h.s. either vanishes if $\psi > \psi_c(\Psi_{p,0})$, or is positive if $\psi < \psi_c(\Psi_{p,0})$, because h is a decreasing function of ψ for fixed Ψ_p. Hence, because of the arbitrariness of $\tilde{t}$, $w_-(t) = 0 \, \forall t$ and thus

$$\psi(t) \geq \psi_c(\Psi_{p,0}) \geq \psi_y(\Psi_{p,0}) \,, \qquad \forall t \,.$$

□

The condition on the constancy of $\tilde{F}(t)$ can be relaxed, if we assume that $\Psi_{p,0} = \psi_0 = 1$, as stated in the following Corollary.

Corollary 4. *If $\psi(0) = 1$ and $\Psi_{p,0} = 1$ and $\tilde{F}(t) \leq \tilde{\tau}/\psi_y(1)$, then $\Psi_p(t) = 1$, $\forall t$ and the solution of Eq. (2.14) is such that $\psi(t) \geq \psi_c(1) \geq \psi_y(1)$.*

Proposition 3 implies, for instance, that in the case of pre-stressed aggregates that have already deformed plastically, during cyclic compression tests at constant load, being $\Psi_{p,0} \geq \psi_0$ at the beginning of every interval of compression (see Proposition 1), then remodelling is not triggered if $\tilde{F}_M \leq \tilde{\tau}/\psi_y(\Psi_{p,0})$ or equivalently, in dimensional form, $F_M \leq 2\pi_0^2 \tau/\psi_y(\Psi_{p,0})$. Indeed for these values of applied constant force the stretch leading to the internal reorganization is never reached, being $\psi(t) \geq \psi_c(\Psi_{p,0}) \geq \psi_y(\Psi_{p,0}) \,, \, \forall t$.
This result can be applied to the description of a cyclic creep test and release in which the force is maintained constant, $F(t) = \tilde{F}_M$, during compression and it is equal to zero during releases. Therefore, when a constant external force $\tilde{F}_M$ is periodically applied and then removed, if $\tilde{F}_M \leq \tilde{\tau}/\psi_y(1)$, no reorganization occurs and the unloaded specimen will go back to the initial configuration, $\psi = 1$, following the classical visco-elastic response, due to the elastic response of cells and the viscous term of the liquid component (see Figure 3, top curve).
The corollary states that if an undeformed aggregate is subjected to compression with bounded force $F(t)$, with maximum below the critical value $\tilde{\tau}/\psi_y(1)$, then the deformation of the aggregate occurs without any plastic effect.
On the other hand, as we shall see in the following proposition, when a constant force $\tilde{F}_M > \tilde{\tau}/\psi_y(1)$ is applied, trajectories enter in the region II identified in Fig. 1, right panel, and the natural configuration of the aggregate changes, so that the solution tends to the intersection between the two curves in Fig. 1, right panel. In this case, when the upper plate is removed the multicellular body does not recover its original shape and a macroscopic deformation can be seen (lower curves in Fig. 3, right panel). The internal reorganization rate depends on the intensity of the load applied to the aggregate, compared to the yield stress and, in particular, it is faster and more intense as $\tilde{F}_M$ increases, as shown in Fig. 3, left panel. In particular we demonstrate the following proposition.

Proposition 5. *If $\tilde{F}_M > \tilde{\tau}/\psi_y(1)$, the solutions of (2.16) starting from $\psi(0) > \dfrac{\tilde{\tau}}{\tilde{F}_M}$ and $\Psi_{p,0} > \psi(0)$, are such that $\psi(t) \in \left[\dfrac{\tilde{\tau}}{\tilde{F}_M}, 1 \right]$ and $\Psi_p(t) \in [\Psi_{p,\infty}, 1]$, where $\Psi_{p,\infty}$ is the solution of (2.22).*

Proof. To prove the thesis we proceed by absurd assuming that there exists a first $\bar{t}$ with

$$\Psi_p(\bar{t}) = \Psi_{p,\infty}\,, \qquad \dot{\Psi}_p(\bar{t}) < 0\,, \qquad \text{and} \quad \psi(\bar{t}) \geq \frac{\tilde{\tau}}{\tilde{F}_M}\,,$$

$$\text{or} \quad \psi(\bar{t}) = \frac{\tilde{\tau}}{\tilde{F}_M}\,, \qquad \dot{\psi}(\bar{t}) < 0\,, \qquad \text{and} \quad \Psi_p(\bar{t}) > \Psi_{p,\infty}\,.$$

In the former case, since $\psi_y(\Psi_{p,\infty}) = \psi_c(\Psi_{p,\infty}) = \dfrac{\tilde{\tau}}{\tilde{F}_M}$, the same reasoning of the previous proposition can be used. If the line $\Psi_p = \Psi_{p,\infty}$ is reached the solution will always stay there. In fact,

$$g(\Psi_p(\bar{t}), \psi(\bar{t})) = g(\Psi_{p,\infty}, \psi(\bar{t})) \leq g\left(\Psi_{p,\infty}, \frac{\tilde{\tau}}{\tilde{F}_M}\right) = \tilde{\tau}\,,$$

which implies that $[g(\Psi_p(\bar{t}), \psi(\bar{t})) - \tilde{\tau}]_+ = 0$ and therefore $\dot{\Psi}_p = 0$, against what assumed.

In the latter case,

$$h(\Psi_p(\bar{t}), \psi(\bar{t})) = h\left(\Psi_p(\bar{t}), \frac{\tilde{\tau}}{\tilde{F}_M}\right) > h\left(\Psi_{p,\infty}, \frac{\tilde{\tau}}{\tilde{F}_M}\right) = \tilde{F}_M \geq \tilde{F}(t)\,,$$

which implies that $\dot{\psi} > 0$, against what assumed.

□

Corollary 6. *If $\tilde{F}(t) = \tilde{F}_M > \tilde{\tau}/\psi_y(1)$, $\forall t$, being the r.h.s of (2.16) continuous and locally lipschitz for ψ and Ψ_p belonging to the compact invariant set $\left[\dfrac{\tilde{\tau}}{\tilde{F}_M}, 1\right] \times [\Psi_{p,\infty}, 1]$, then solutions of (2.16) will tends to the stationary point $\left(\dfrac{\tilde{\tau}}{\tilde{F}_M}, \Psi_{p,\infty}\right)$, where $\Psi_{p,\infty}$ is the solution of (2.22).*

Corollary 6 states that, when the aggregate is compressed with a constant force, the stationary stretch, in dimensional terms, is given by $\psi_\infty = \dfrac{2\tau\pi R_0^2}{F_M}$, where $F_M = \max_t\{\tilde{F}_{appl}(t)\}$. From the experimental point of view this allows to determine the value of the yield stress from a compression test at constant load measuring the steady state stretch, i.e., $\tau = \dfrac{F_M}{2\pi R_0^2}\psi_\infty$.

The results demonstrated in Proposition 3 and 5 are also evident plotting the vector field corresponding to (2.16). Indeed, if $\tilde{F} \leq \tilde{\tau}/\psi_y$ (see Figure 1, left panel), ψ and Ψ_p will tend to the grey curve, which corresponds to the condition $h(\Psi_p, \psi) = \tilde{F}_M$. Then the solutions of the system (2.16) starting from $\psi(0) = 1$ and $\Psi_p(0) = 1$, will keep $\Psi_p = 1$ while ψ will tend to $\psi_c(1)$. On the other hand if $\tilde{F}_M > \tilde{\tau}/\psi_y(1)$ (see Figure 1, right panel), ψ and Ψ_p will tend to the the intersection of the gray and black curve, which represents the solution of the system (2.21).
We remark that the condition $\tilde{F}_M > \tilde{\tau}/\psi_y(1)$ is coherent with the one found in [10] for creep tests at constant stress. Indeed, defining the yield stress $P^*_{appl} = \tilde{F}_M\psi_y(1)/(\pi R_0^2)$, the creep test yield condition becomes $P^*_{appl} = 2\tau$.

Also in the case of a cyclic test, it is possible to see that the steady state stretch and the maximum internal reorganization that can be induced depend on the intensity of imposed loads and do not tend to the trivial state, i.e., $\Psi_p \to 0$ and $\psi \to 0$, in contrast with what shown in [10]. This means that, as remodelling takes place, cellular aggregates reorganize (i.e., Ψ_p decreases) in order to bear the load. Moreover being ψ decreasing, the external stress P_{appl} generated by a constant force, decreases in time.

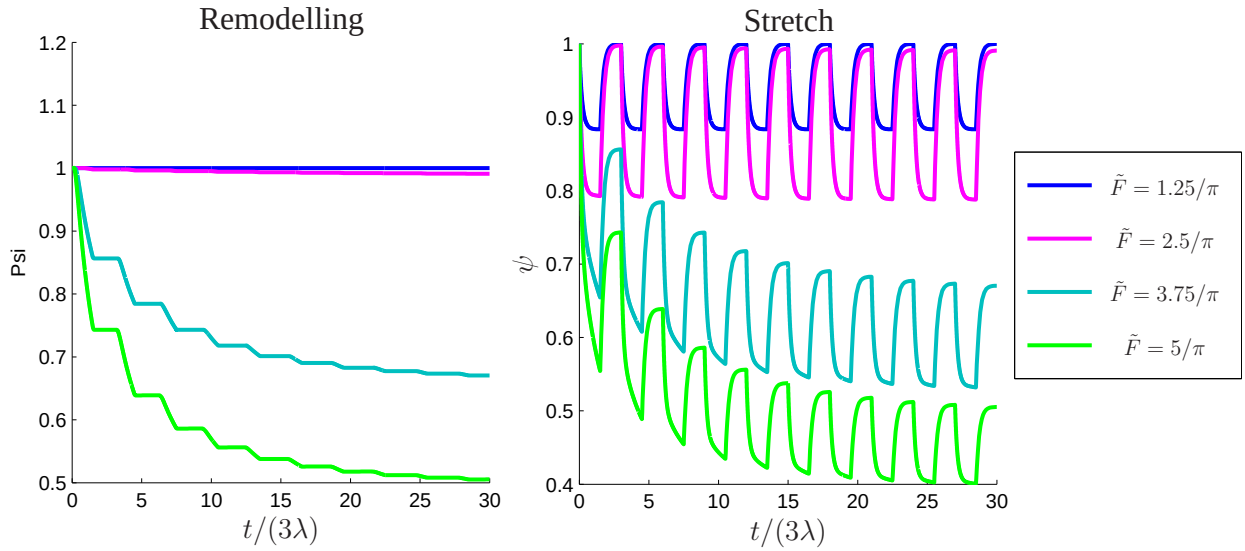

Figure 3: Cycle of compressions, when a constant external force $\tilde{F}_M$ is periodically applied and then removed: reorganization (on the left) and stretch (on the right). The simulations are performed setting $\tilde{\tau} = 0.625$ and $\tilde{\mu} = 1.6$. The compression and release times are both equal to $\tilde{t}_c = \tilde{t}_r = 3/2$. From top to bottom the applied force increases.

4. Conclusions

In this work we discuss some analytical properties of the solution of the system proposed in [10] to describe cellular aggregates compression. We focus on the case in which the biological specimen is deformed under a controlled force. Numerical results are proposed for the specific case in which the imposed force is kept constant in time and for a cycle of compression at constant force and subsequent releases. These conditions were not exploited in [10], where the main focus was the description of compression at constant deformation, for which biological experiments are present in literature, and the study of creep tests under constant imposed stress. However, one of the simplest test that can be done on a specimen in order to assess its mechanical response is the imposition of a constant load on it. Therefore, using the same apparatus presented in [7], the numerical results proposed here can be easily validated, imposing different forces on the upper plate of a cylindrical sample of biological material and monitoring the deformation experienced by

the specimen. Moreover, in order to test the remodelling occurring inside the aggregate, the upper plate should be lifted up and the shape recovery of the sample monitored.
The results reported in this work, highlight that, when the force (and not the stress) is maintained constant, even if the load is initially able to trigger the rupture of adhesive bonds, cells re-allocate in order to increase the transverse section and to reach a new internal configuration that does not undergo reorganization under the same imposed load. The final stretch reached by the aggregate depends on the imposed load and on reorganizing properties (i.e., τ) of the cellular structure, but it is independent from μ.
Thanks to Corollary 6, it is possible to determine the value of the yield stress from a compression test at constant load of an aggregate, simply measuring the steady state stretch, ψ_∞. Indeed, in dimensional terms, $\tau = \dfrac{F_M}{2\pi R_0^2}\psi_\infty$.
However we have to be aware that some simplifications (on the geometry of the sample that is usually spherical, on the type of deformation experienced) have been done in order to obtain equations that can be analytically studied.
Furthermore, more realistic 2D and 3D simulations of aggregates deformation, considering more complex aggregate shapes, should be performed, in order to obtain a more precise calculation of non-homogeneous deformation occurring inside living structures. Future works should focus on the derivation of the remodelling equation (2.7) directly from measurements of cell-cell bond rupture, incorporating in the macroscopic model information deriving from the subcellular scale.

References

[1] D. Ambrosi, F. Mollica. *On the mechanics of a growing tumour.* Int. J. Engng. Sci., 40:1297-1316 (2002).

[2] D. Ambrosi, F. Mollica. *The role of stress in the growth of a multicellular spheroid.* J. Math. Biol., 48:477-499 (2004).

[3] D. Ambrosi, L. Preziosi. *Cell adhesion mechanisms and stress relaxation in the mechanics of tumours.* Biomech. Model. Mechanobiol., 8:397-413 (2009).

[4] D. Ambrosi, K. Garikipati, E. Kuhl. *Mechanics in biology: Cells and tissues*. Phil. Trans. R. Soc. A, 367:3333-3334 (2009).

[5] D. Ambrosi, L. Preziosi, G. Vitale. *The insight of mixtures theory for growth and remodeling*. Z. Angew. Math. Phys., 61: 177–191 (2010).

[6] D. Ambrosi, L. Preziosi, G. Vitale. *The Interplay between Stress and Growth in Solid Tumors.* Mech. Res. Comm., 42: 87-91 (2012).

[7] G. Forgacs, R.A. Foty, Y. Shafrir, M.S. Steinberg. *Viscoelastic properties of living embryonic tissues: A quantitative study.* Biophys. J., 74:2227-2234 (1998).

[8] R.A. Foty, G. Forgacs, C.M. Pfleger, M.S. Steinberg. *Liquid properties of embryonic tissues: Measurement of interfacial tensions.* Phys. Rev. Lett., 72:2298-2301 (1994).

[9] R.A. Foty, G. Forgacs, C.M. Pfleger, M.S. Steinberg. *Surface tensions of embryonic tissues predict their mutual envelopment behavior.* Development, 122:1611-1620 (1996).

[10] C. Giverso, L. Preziosi. *Modelling the compression and reorganization of cell aggregates*, Math. Med. Biol., 29(2):181-204 (2012).

[11] A. Grillo, C. Giverso, M. Favino, R. Krause, M. Lampe, G. Wittum. *Mass Transport in Porous Media with Variable Mass*. Numerical Analysis of Heat and Mass Transfer in Porous Media. A. Oechsner, L.F.M. da Silva, H. Altenbach Eds. Springer Verlag Germany (2012).

[12] A. Iordan, A. Duperray, C. Verdier. *Fractal approach to the rheology of concentrated cell suspensions.* Phys. Rev. E, 7:011911 (2008).

[13] L. Preziosi, D. Ambrosi, C. Verdier. *An elasto-visco-plastic model of cell aggregates*. J. Theor. Biol., 262:35-47 (2010).

[14] L. Preziosi, G. Vitale. *A multiphase model of tumour and tissue growth including cell adhesion and plastic re-organisation.* Math. Mod. Meth. Appl. Sci., 21: 1901-1932 (2011).

[15] L. Preziosi, G. Vitale. *Mechanical aspects of tumour growth: Multiphase modelling, adhesion, and evolving natural configurations*, in M. Ben Amar, A. Goriely, M. M. Müller, L. F. Cugliandolo, Eds., New Trends in the Physics and Mechanics of Biological Systems, Lecture Notes of the Les Houches Summer School, 92: 177-228, Oxford University Press (2011).

[16] J. Humphrey, K. Rajagopal. *A constrained mixture model for growth and remodeling of soft tissues.* Math. Mod. Meth. Appl. Sci., 22:407-430 (2002).

[17] J. Humphrey, K. Rajagopal. *A constrained mixture model for arterial adaptations to a sustained step change in blood flow.* Biomech. Model. Mechanobiol., 2:109-126 (2003).

[18] E.K. Rodriguez, A. Hoger, A. McCulloch. *Stress-dependent finite growth in soft elastic tissues*. J. Biomech., 27:455-467 (1994).

[19] L.A. Taber, J.D. Humphrey. *Stress-modulated growth, residual stress, and vascular heterogeneity*. J. Biomech. Eng., 123:528-535 (2001).

[20] G. A. Truskey, F. Yuan, D.F. Katz. *Transport Phenomena in Biological Systems.* Prentice Hall (2009)

[21] A. Vaziri, A. Gopinath. *Cell and biomolecular mechanics in silico*. Nat. Materials, 7: 15–23 (2008).

[22] C. Verdier, J. Etienne, A. Duperray, L. Preziosi. *Review: Rheological properties of biological materials*. C. R. Phys., 10:790-811 (2009).

[23] B.S. Winters, S.R. Shepard, R.A. Foty. *Biophysical measurement of brain tumor cohesion.* Int. J. Cancer, 114:371-379 (2005).